Synthesis of New Organo-Inorgano-Clay MaterialsBased on Metal Ions, CTMAB, and Bentonite. Application for Removal of Acid Dye

Dali, Nacer; Ouadjenia, Fatima; Marouf, Reda*[+]

Department of Chemistry, Faculty of Exact Sciences, Mustapha Stambouli University of Mascara, Laboratory of Materials, Applications and Environment, Po Box 305 Mamounia Road, Mascara 29000, ALGERIA

ABSTRACT: *The present study focuses on the synthesis of pillared bentonite materials prepared by intercalating solutions of aluminum, chromium, iron, and. cetyltrimethylammonium bromide (CTMAB) into natural bentonite. Six solids were obtained and applied as adsorbents to remove acid-yellow E-4G dye from aqueous solutions. Different characterization methods, such as chemical composition, X-ray diffraction, and specific surface area, were used for that purpose. The efficiency of dye removal was studied as a function of pH, initial dye concentrations, contact time, and temperature. The efficiency of dye removal by CTMA-Al intercalated bentonite was found higher than that of inorgano-bent, under similar conditions. The results obtained showed that the maximum adsorption capacity for dye by modified bentonite was reached within the pH range from 1 to 2. Indeed, the maximum adsorption capacity was estimated to be 385 mg/g at room temperature. The results of the kinetic study regarding the removal of E-4G dye by modified bentonites was found to fit the pseudo-second-order model. Moreover, it turned out that the adsorption isotherm data obtained fit well the Freundlich model, which is not the case for the Langmuir and D-R models tested. Calculated thermodynamic parameters indicated that the adsorption process is spontaneous and endothermic with bentonite intercalated by aluminum and iron (B-AlFe) and is exothermic in the case of inserted bentonite by cetyltrimethylammonium and chromium (B-C-AlCr).*

KEYWORDS: *Bentonite; Aluminum(III); Chromium(III); Iron(III); Cethyltrimethylammonium bromide; Dye adsorption.*

INTRODUCTION

The demand for natural clay minerals is on a constant rise in the industrial field and in scientific research. This is mainly due to their availability in large quantities as well as to their valuable properties such as ion exchange capacity, catalyst, and adsorption. It is worth noting that bentonite clay which contains essentially montmorillonite (Mt), is widely abundant in nature. Bentonite clays are aluminosilicates that have a 2:1 layer structure which consists of an alumina octahedral layer located between two silica tetrahedral layers. In many countries,

***To whomcorrespondenceshouldbeaddressed.*

+E-mail: *r.marouf@univ-mascara.dz*

1021-9986/2022/2/431-445 15/$/6.05

large deposits of natural bentonite provide significant advantages to local industries which can treat wastewater contaminated by various pollutants at a low cost [1]. Over the last few years, the use of bentonite as an adsorbent for many adsorbates has widely been investigated [2-4]. However, this type of clay inherently presents the disadvantage of poor access to its active sites, hence decreasing its adsorption capacity or catalytic power. Chemical modifications in the structure with cationic surfactants and certain polyhydroxyl cations were also carried out for the purpose of improving their adsorption capacity [5]. It has been reported that the intercalation of some metals such as aluminum [6] iron [7] and titanium [8] and some surfactants like CTMA [9] in 2:1 clay minerals significantly increases the sorption efficiency. Moreover, researchers have reported also the simultaneous insertion of two metals in bentonite i.e. Al/Fe-bent [7] and Fe/Cr-bent [10]. In addition, the occupation of exchange sites on the surface of bentonite by ammonium surfactant cations, such as cethyltrimethylammonium, changes the surface properties from hydrophilic to hydrophobic [11].

In the present work, an attempt is made to take advantage of the benefits of inserting mixed polycations as inorganic pillars and the CTMA, which is an organic intercalation component, into bentonite; the performances of the two adsorbents are then compared. The specificity of this study is the combination of both inorganic and organic intercalants inserted at the same time in a single adsorbent. In addition, we worked with the three most widely used polycations (Cr, Al, Fe) in the literature mixed together. For this reason, there has been much interest in the use of modified bentonites as adsorbents to prevent and fight the organic contaminants encountered in the environment.

Over the last few years, synthetic dyes have been increasingly used in textile industries and consequently, large quantities of dye wastewater have been generated. It isestimated that 10,000 tons of dye wastewater effluents are discharged annually into the environment and around 50% of these dyes are azo dyes which are organic compounds bearing the functional group R−N=N−R′, in which R and R′ are usually aryl [12]. The presence of dyes or their degradation products in water, even at very low concentrations, can also cause human health disorders such as nausea, hemorrhage, and ulceration of the skin and mucous membranes [13].

Toxic substances contained in dye wastewater should therefore be completely removed before being released into the environment. The physicochemical dye wastewater treatment techniques currently available such as plasma [14], adsorption by nanofibres [15, 16], emulsion liquid membrane [17], coagulation/flocculation [18] oxidation [19], and photocatalytic [20] are not always reliable for many reasons. Sometimes, they are too expensive and not easy to implement. Actually, several previously conducted research studies have shown that the adsorption of dyes on different adsorbents such as nano-zerovalent iron [21, 22], zeolite-x [23], and activated carbon [24] present high removal efficiency, but the uptake of dyes on modified clay minerals can be regarded as a valid and promising alternatives to these physicochemical methods.

The aim of the present investigation is to elaborate on two kinds of intercalated bentonite materials, namely inorgano-bent and inorgano-organo-bent, and then try to compare the efficiencies of the obtained adsorbents towards the adsorption of acid yellow E-4G from an aqueous solution. The inorgano-bent adsorbent was prepared with natural bentonite clay, brought from the deposit of M'zila, a region in the Wilaya of Mostaganem (northwestern Algeria), which was first pillared with chromium and iron polycations solutions and then mixed with intercalating Al/Cr and Al/Fe solutions. The organo-inorgano-bent was obtained using cethyltrimethylammonium cation mixed with intercalating solution based on aluminum and chromium.

Various analytical techniques, such as XRD, specific surface area, and chemical composition, were applied for the purpose of examining and identifying the samples before and after modification. In order to prepare the sorbents samples, raw bentonite was first purified and then subjected to the intercalation procedure. The effects of the pH medium, initial dye concentrations, contact time, and temperature on the efficiency of dye removal were carefully investigated. Moreover, the adsorption isotherms, kinetics, and thermodynamics of the adsorption process were also examined.

EXPERIMENTAL SECTION

Materials

The bentonite used is locale clay obtained from Mostaganem, Algeria. This clay is manufactured by BENTAL factory. Before the experiments, the samples

were purified and sieved at 80 µm. All reagents, i.e. $AlCl_3$, $FeCl_3$, $CrCl_3$, $BaCl_2$, $CaCl_2$, NaCl, KNO_3, $AgNO_3$, NaOH and HCl, were of analytical grade.

Preparation of hydroxy-cation solution

Three polycations solutions, based on aluminum, iron, and chromium were prepared in this study. A volume of 200 mL of 0.2 M NaOH solution was added slowly to 100 mL of 0.2 M M-Cl_3 solution (M is either Al, Fe, or Cr) under vigorous stirring at 60°C, until a final hydrolysis ratio of OH^-/M^{3+} = 2 was reached. Then the solution obtained was allowed to age for 72 h [25].

Preparation of pillared bentonite

Two methods were introduced to prepare the pillared bentonite PILB. First, the three pillaring solutions were taken separately and added to the bentonite; they were kept under stirring for 4 hours at 70 °C, at the ratio of 50 mmol oligomeric cations per gram of bentonite [26]. Then the pillaring solutions were first mixed in 1:1 proportion and then added to the bentonite. The mixed pillaring solutions obtained are Al/Fe and Al/Cr. Afterward, the resulting slurry was stirred for 24 h at room temperature, filtered, and repeatedly washed with deionized water. The resulting solids were then dried at 80 °C and kept in a sealed bottle. The ensuing pillared bentonites were designated as B-Fe, B-Cr, B-AlFe, and B-AlCr.

Preparation of CTMA-PILB

Cetyltrimethylammonium bromide (CTMA) whose chemical formula is $C_{19}H_{42}NBr$ and molecular weight is 364.45 g/mol, was supplied by Merck, Germany. An amount of 1 g of bentonite was first dispersed in 100 mL of distilled water, and kept for 24 h at room temperature, under vigorous agitation. CTMAwas first intercalated into the bentonite in order to synthesize organoclay; then, the polycation solution was added to the CTMA-B [27]. The amount of 175 mg of CTMA was considered in our case. This quantity, which is equivalent to one time of the Cation Exchange Capacity (CEC) of bentonite, was slowly added to the mixture at 60 °C [28]. The polycation solutions used are that of Alaloneand that of Almixed with Cr. After 4 hours of stirring, the organo-inorgano-clays were filtered, washed with distilled water several times, and oven-dried at 80 °C. The solids obtained were designated as B-C-Al and B-C-AlCr.

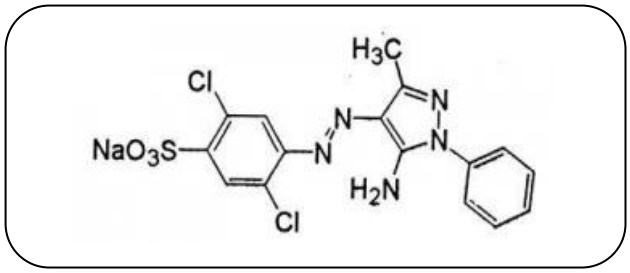

Fig. 1. Molecular structure of bemacid E-4G.

Dye

Bemacid yellow E-4G (C.I. Acid Yellow 49) was supplied by SOITEX, a textile factory (Tlemcen, Algeria). This dye is manufactured by CHT, Switzerland Company. The dye solution was prepared by dissolving 1 g of dye in 1 L distilled water from which dilute solutions were realized at desired concentrations. The chemical formula and molecular weight of E-4G are $C_{16}H_{13}Cl_2N_5O_3S$ and 426.24 g mol^{-1}, respectively. The molecule structure of the dye molecule is shown in Fig. 1.

Properties and characterization of adsorbents

The adsorption properties measured are acidity, $pH_{(PZC)}$, Cation Exchange Capacity (CEC), and specific surface area. The acidity was assessed as follows: 1 g of the sample was added to 10 mL of calcium chloride ($CaCl_2$) solution at 0.01 M, kept under agitation for 10 min, and allowed the solution to stand for two hours before measuring its pH. The zero charge point ($pH_{(PZC)}$) was measured as follows: a series of 20 mL of 0.01 M KNO_3 solution was placed in a closed Erlenmeyer flask. Their pH value was adjusted in the range from 2 to 10, by the addition of 1 M HCl or 1 M NaOH solutions. Next, 0.1 g of each bentonite sample was added and agitated for 24 h, under atmospheric conditions. When the final pH was determined, the evolution of ΔpH (final pH–initial pH) was plotted as a function of the initial pH. The $pH_{(PZC)}$ is the point where the ΔpH versus pH initial curve crosses line zero [29].

As for the Cation Exchange Capacity (CEC) tests, they were performed by the conductimetric titration method. This method consists of saturation of the sample with $BaCL_2$ solution [30]. In addition, the surface area was estimated according to Sears' analytic method [31]. A quantity f 0.5 g of the sample was mixed with 50 mL of 0.1N HCl and10 g of NaCl. The mixture obtained, with pH= 3, was then titrated with standard 0.1M NaOH

in a thermostatic bath at 25 °C to pH 4, and then to pH 9. The volume, *V*, required to raise the pH from 4 to 9 was noted and the surface area was computed from the following equation:

$$S\left(m^2/g\right) = 32V - 25 \quad (1)$$

The chemical analysis of natural bentonite (BN) was performed using an X-fluorescence XRF instrument, Thermo scientific ARL 9900 series. X-ray analyses were achieved by D8 Advance Brucker diffractometer employing copper Kα radiation (λ= 0.154 nm) operating at 40 kV and 40 mA with a fixed slit. The scan rate was 1.0° (2θ) min^{-1} and the scanning scope varied from 2° to 60° (2θ). The residual concentrations of dyes were detected using spectrophotometer Model VIS 7220 G, (Biotech Engineering Management).

Batch experimental procedure

Batch experiments were carried out by mixing 20 mL of bemacid yellow E-4G solutions of known concentrations with 0.02 g of intercalated bentonite. The mixtures were then agitated at room temperature (25 °C). Various parameters such as the contact time (2–120 mins), pH of the medium (1–9), and temperature (30, 40, and 50°C) were considered for optimizing the experimental conditions. The pH of the medium was adjusted using 1 M HCl and 1 M NaOH solutions. The experiments were carried out under agitation time for 3h, a period that was determined from the effect of the contact time experiment. Afterward, the mixtures were filtered and the filtrates were analyzed for their E-4G content using UV-Vis at a wavelength of 400 nm. The amount of dye adsorbed per gram (mg/g), was calculated using the expression below:

$$q_e = \frac{(C_0 - C_e)}{m} V \quad (2)$$

where C_0 and C_e are the initial and the equilibrium dye concentrations (mg/L), *V* is the volume of dye solution used (L), and *m* is the mass of material used (g).

RESULTS AND DISCUSSIONS

Characterization of raw and modified bentonite

The chemical composition (wt %) of raw bentonite is as follow: SiO_2 (64.22), Al_2O_3 (11.62), CaO (9.33), Fe_2O_3 (4.88), MgO (3.47), Na_2O (3.38), TiO_2 (1.06), SO_3 (0.46), P_2O_5 (0.03) and loss on ignition (1.55). This suggests the presence of high proportions of silica, alumina, and lime in the sample, while iron, magnesium, sodium, titanium, sulphate, and phosphor oxides are present in low percentages.

The characteristics of the adsorbents are shown in Table 1. The pH values of all materials in the solution were under pH= 7, except for natural bentonite BN. Also, B-Fe and B-Cr showed a more pronounced acidic behavior as compared to the other samples. This result suggests that there is the liberation of protons during oligomerization [10]. According to the $pH_{(PZC)}$ experience, the insertion of polycations into bentonite causes the $pH_{(PZC)}$ values to decrease round to pH 4 and 5, which is not the case for raw bentonite. The $pH_{(PZC)}$ values for B-C-Al and B-C-AlCr are equal to 6.40 and 5.49, respectively. In all cases, the inorgano-bentonite or inorgano-organo-bentonite samples present a positive surface charge in an acidic medium.

The calculated CEC values reveal that the insertion of polycations or CTAB in bentonite increases considerably the cation exchange capacity whose maximum values were registered for B-AlCr and B-C-Al. The same observation was reported about the specific surface area values. Comparing the effect of inserting the three polycations solutions, it was found that the insertion of chromium into bentonite was the most beneficial since the best results on CEC and specific surface area were attributed to B-AlCr sample.

The X-ray diffraction patterns of the samples are illustrated in Figs. 2 and 3. The X-ray diffractogram of natural bentonite (BN) presents a d_{001} peak, characteristic of montmorillonite, at 2θ = 8.07° (d=1.27 nm) and another one, typical of illite, at 2θ = 10.3°. That does not mean that raw bentonite contains only clay minerals but also quartz, calcite, and dolomite as well. The hydroxy-metal polycations exchange increases the value of d_{001}; the maximum distance was reported with the B-AlFe sample (d = 1.62 nm). In addition, it was revealed that the basal spacing of B-Cr was larger than that of B-Fe; also, the Mt peak of B-AlFe was higher than that of B-AlCr. It is clear that the addition of aluminum into bentonite as intercalant has a very remarkable effect as compared to the other metals and its performance can be improved by mixing it with iron or chromium. The diffractograms of B-Cr and B-Fe depicted in Fig. 3 show clearly that the intensity of the d_{001} diffraction peak was reduced, which may be attributed to the delamination of Mt layers by ions. This reduction of the peak intensity observed in diffractograms

Table 1. Characteristics of modified bentonite sorbents

Property	BN	B-Fe	B-AlFe	B-Cr	B-AlCr	B-C-Al	B-C-AlCr
Acidity	7.28	4.01	5.60	3.49	4.79	5.03	4.98
PZC	8.3	4.4	6.20	3.5	5.8	6.40	5.49
CEC (meq/100g)	48	96	112	110	159	131.12	119.2
Specific Surface ($m^2\ g^{-1}$)	45.5	119	123.4	77.4	141.4	122.2	103
Distance basal d (Å)	12.7	13.49	16.22	14.19	15.32	18.52	17.60

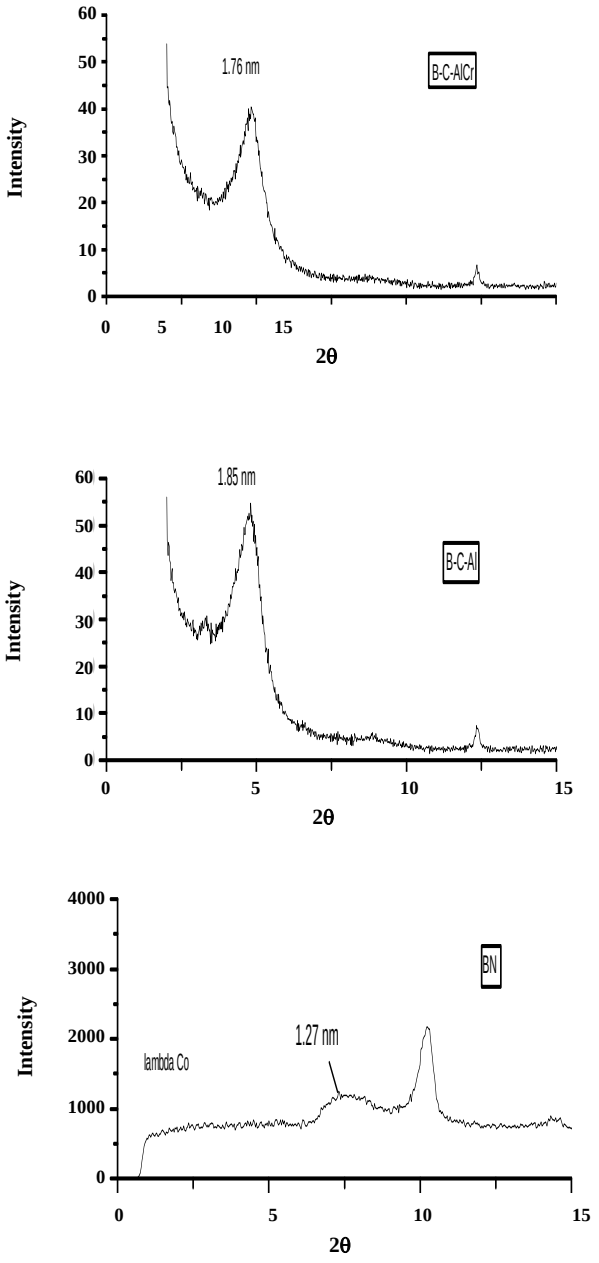

Fig. 2: XRD patterns of BN, B-C-Al and B-C-AlCr materials.

might also be attributed to the collapse of the montmorillonite layers due to the partial incongruent phase transition of hydroxy-Al into Fe/Al or Cr/Al oxides and their interactions during aging and drying, as suggested by *Thomas et al.*[32].

The incorporation of a surfactant, such as CTMA, in bentonite, leads to a considerable increase in the thickness of the clay mineral sheet; this thickness is equal to1.85 nm for B-C-Al. This value is more than that of the solid B-CTMA (d=1.76 nm), which has been cited in our previous work [9], and less than that found by *Guo et al.* (d = 2.1 nm) [33] who used 10CTAB for bentonite intercalation. However the addition of CTA^+ ions alone or mixed with aluminum or chromium polycation solutions between the montmorillonite layers helps to increase the basal spacing of the sheet.

Effect of pH

Fig. 4 clearly illustrated the amounts of E-4G adsorbed onto pillared bentonites at various pH values. As depicted in that figure, the variations of E-4G amounts adsorbed on all our materials as a function of pH have the same shape. It is worth noting that the amounts adsorbed are high for very low pH values but they start decreasing significantly above the pH= 6. This result is in agreement with $pH_{(PZC)}$ value found before; in this case, the E-4G dye is anionic in solution and is therefore absorbed by the samples of bentonite which develops a positive charge on its surface in an acidic medium.

In bentonite-aqueous solution system, the potential of the surface is determined by the acidity of H^+ ions, which reacts with the bentonite surface. For the bentonite mineral, the potential determining are H^+ and OH^- and complexions formed by bonding of H^+ and OH^- [34].

At low pH the reaction is:

$$Me-OH + H^+ \rightarrow Me-OH^{2+} \quad (3)$$

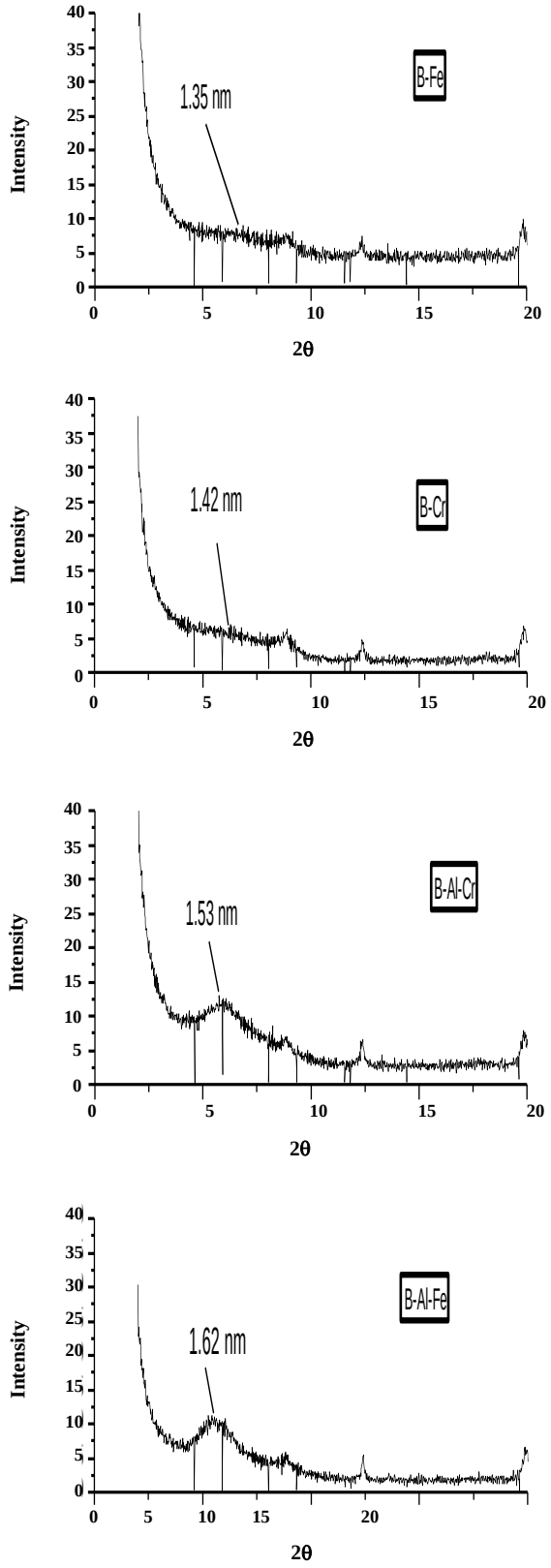

Fig.3: XRD patterns of BN, B-C-Al, and B-C-AlCr materials.

At high pH the reaction is:

$$Me-OH^- \rightarrow Me-O + H_2O \quad (4)$$

This implies that the highest amount of dye is adsorbed at weak pH values, that is to say when the adsorbent and adsorbate develop electric charges of opposite signs [35]. Moreover, this same figure allows observing a rapid decrease in the quantity of dye adsorbed beyond the value pH = 2 for the samples B-Cr, B-Fe, B-AlFe, and B-AlCr; however, for B-C-Al and B-C-AlCr, the decrease of $q_e$is less intense. Indeed, one can clearly note that the curves form practically a plateau for pH values between 2 and 7; q_e decreases significantly afterward. The change in pH in E-4G solution had a slight influence on the adsorption capacity for B-C-Al and B-C-AlCr. The exchangeable cations (Na^+, Ca^{2+}, etc.) present in Mt interlayers are strongly hydrated in the presence of the water, resulting in a hydrophilic environment at the bentonite surface. When adding $CTMA^+$ ions to bentonite structure the Na^+ and Ca^+ ions will be substituted by those of $CTMA^+$, resulting in a change in bentonite surface from hydrophilic to hydrophobic.

These results are in agreement with the works realized on the adsorption of methyl orange and indigo carmine by hexadecyl pyridinium-modified clay [36] and on the adsorption of remazol blue by ethylenediamine-modified bentonite [37].

The addition of CTMA allows the bentonite to have a wider pH range (from 1 to 7) for adsorbing the dye; this can be very practical if the adsorption takes place at pH values similar to those of wastewater from the textile industry. The pH value is fixed between 1 and 2 for the coming experiments.

Adsorption isotherms

The adsorption isotherms were realized at different initial concentrations (30-70 mg/L for B-Cr and B-Fe, 100-400 mg/L for the others) during a period 3 hours, at ambient temperature, the adsorbent dose was 1 g/L, and the pH values were between 1 and 2. The isotherms representing the amount of E-4G adsorbed as a function of equilibrium concentration, are neatly plotted. The adsorption isotherms of dye onto the pillared bentonites are presented in Figs. 5 and 6. It is explicitly shown that the amount of dye adsorbed increases as the equilibrium dye concentration rises. According to the classification of *Giles et al.* [38],

isotherms have the S-shape except those of B-C-Al and B-C-AlCr which shows an L-shape. The S-form means that the adsorption is cooperative since the adsorbed molecules facilitate the adsorption of the other molecules; however, the L-isotherm entails a gradual saturation of the solid. The maximum amount of E-4G adsorbed was 385.25 mg/g attributed to the B-C-Al sample which showed a removal efficiency of 96%. However, the amounts of dye adsorbed onto B-Fe and B-Cr were almost identical (61.39 and 60.03 mg/g). So the inorgano-organo-bentonite sample has a more significant adsorption capacity than inorgano-bentonite, under the same operating conditions.

The equilibrium adsorption capacity of dye onto B-C-Al was more than the values reported in the literature towards the adsorption of RB19 dye onto didodecyldimethylammonium bromide modified bentonite (335 mg/g) [39] and CTAB-Bent was used for adsorption of weak acid scarlet (175.44 mg/g) [33] and Rhodamine B dye (173.5 mg/g) [40].

The Langmuir and Freundlich equations expressed by the Eqs. (5) and (6) respectively were used for modeling the adsorption data [41, 42].

$$q_e = \frac{Q_0 K_L C_e}{1 + K_L C_e} \quad (5)$$

$$q_e = K_F C_e^{\frac{1}{n}} \quad (6)$$

Where Q_0 is the maximum adsorption capacity (mg/g) and K_L (L/mg) is Langmuir adsorption constant. K_F and n are the Freundlich constants, indicating the capacity and intensity of adsorption, respectively.

Eqs (5) and (4) can also be represented by the linear forms below:

$$\frac{C_e}{q_e} = \frac{C_e}{Q_0} + \frac{1}{K_L Q_0} \quad (7)$$

$$\log q_e = \log K_F + \frac{1}{n} \log C_e \quad (8)$$

The Dubinin-Radushkevich (D–R) isotherm model is valid at low concentration ranges; it can be used to describe adsorption on both homogeneous and heterogeneous surfaces [43, 44]. The linear form of the D-R equation is as follows:

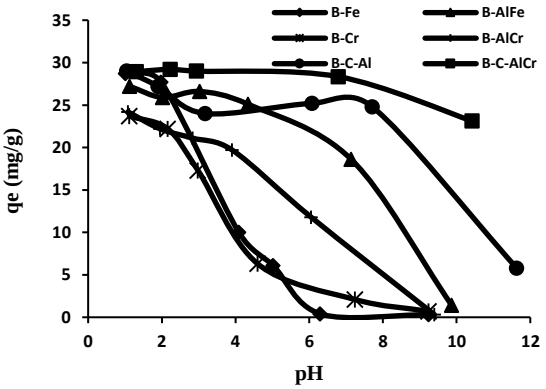

Fig. 4: Effect of pH for the adsorption of E-4G onto modified bentonites.

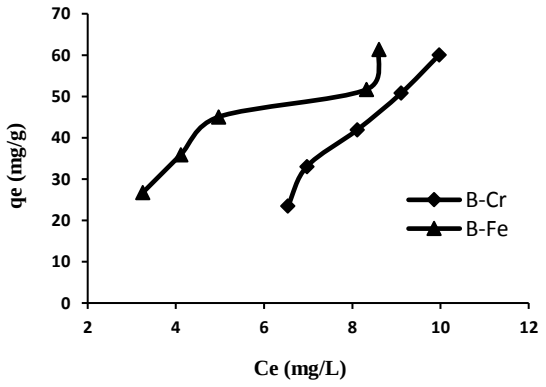

Fig.5: Adsorption isotherms of E-4G onto B-Fe and B-Cr.

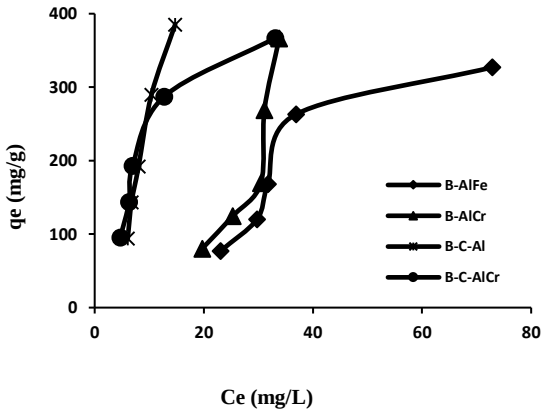

Fig. 6: Adsorption isotherms of E-4G onto modified bentonite.

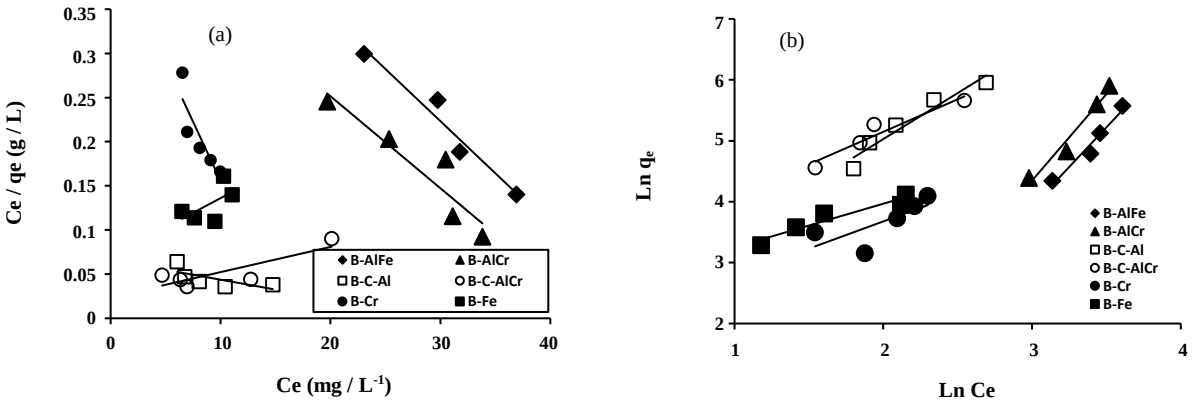

Fig.7: Linearized adsorption isotherms of (a) Langmuir and (b) Freundlich.

$$\ln q_e = \ln q_{max} - \beta \left[R\,T \ln\left(1 + \frac{1}{C_e}\right)\right]^2 \quad (9)$$

Where q_{max} (mg/g) is the saturation adsorption, the value of β is related to the adsorption of free energy. R is the ideal gas constant (8.31 J/mol.K), and T is the solution temperature (K). The value of mean sorption energy, E (J/ mol), can be calculated from D–R parameter β as follows:

$$E = \frac{1}{\sqrt{2\beta}} \quad (10)$$

The value of E(kJ/mol) gives information about the type of adsorption mechanism as chemical ion exchange or physical adsorption. A value of E between 8 and 16 kJ/mol corresponds to chemical ion-exchange processes. In the case of E< 8 kJ/mol, the adsorption mechanism is governed by physical sorption and it may be dominated by particle diffusion if E>16 kJ/mol [45].

The constants obtained from Langmuir, Freundlich, and D-R models are summarized in Table 2. The Langmuir and Freundlich plots corresponding to the adsorption of E-4G onto modified bentonites are given in Fig. 7. The regression coefficient values (R^2) for Freundlich isotherm were above 0.90, indicating a very good mathematical fit by this model. When the values of 1/n are greater than the unit, the adsorption of dye should occur in a multi-molecular manner where more than one molecule is adsorbed per adsorption site. The Langmuir model does not fit the experimental data because the Q_0 values are insignificant and those of R^2were very low (between 0.34 and 0.87). This finding may be explained by the fact that the Langmuir equation is valid for monolayer adsorption onto a surface containing a finite number of identical sites, while Freundlich isotherm fits satisfactorily the sorption data on heterogeneous surfaces.

The D-R isotherm describes well the data of E-4G adsorption on modified bentonites because the R^2 were all above 0.93 except for the B-AlCr sample. It is also noted that q_{max} values obtained by D-R model are different from q_e obtained by the experience. The values of E were between 0.116 and 0.198 kJ mol^{-1}, which are less than 8 kJ/mol, this implies that the adsorption process of E-4G dye on modified bentonite adsorbents follows physical adsorption.

Fig. 8 illustrated the effect of the temperature on the adsorption of E-4G onto the B-AlFe and B-C-AlCr. The isotherms realized at 30, 40 and 50 °C are S-type according to the *Giles et al.* classification. The amounts of dye adsorbed on both adsorbents at different temperatures are similar and no significant change was noted except for a slight increase at a temperature of 50°C.

Adsorption kinetics

Various kinetic models including the first-order, pseudo-second-order, and intraparticle diffusion were used to test the experimental data in order to determine the adsorption mechanism. It was revealed that the adsorption of E-4G dye on all six adsorbents increases with time and reached equilibrium at 60 min as shown in Fig. 9. The adsorption rates of the E-4G on intercalated bentonites are rapid early in the process and then become slower over time. The average dye removal efficiency of our adsorbents was found around 81% after 25 min of contact time.

Table 2: Isotherms constants of E-4G adsorption onto modified bentonite samples.

Model	B-Fe	B-Cr	B-AlFe	B-AlCr	B-C-Al	B-C-AlCr
Langmuir						
Q_0(mg g^{-1})	166.66	-38.46	-90.09	-100.0	-500.0	1000
K_L(L mg^{-1})	0.084	0.061	0.019	0.021	0.030	0.032
R^2	0.344	0.762	0.953	0.863	0.480	0.874
Freundlich						
1/n	0.716	1.614	2.597	2.838	1.509	1.067
K_F (mg g^{-1}(L mg^{-1}) $^{1/n}$)	12.604	1.165	0.020	0.015	7.441	20.328
R^2	0.908	0.978	0.959	0.967	0.937	0.926
Dubinin-Radushkevich						
Q_m (mg g^{-1})	66.48	120.90	417.79	550.04	529.01	361.04
β(mol^2 kJ^{-2})	12.65	77.60	957	832.2	72.05	36.95
E (kJ mol^{-1})	0.198	0.080	0.023	0.025	0.083	0.116
R^2	0.964	0.972	0.930	0.815	0.994	0.980
qe_{exp} (mg g^{-1})	61.39	60.03	327.1	366.18	385.25	366.89

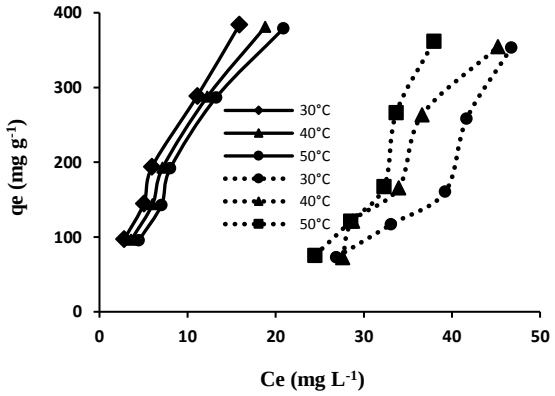

Fig.8: Adsorption isotherms of E-4G onto B-C-AlCr (—) and B-AlFe (- · -) at different temperatures.

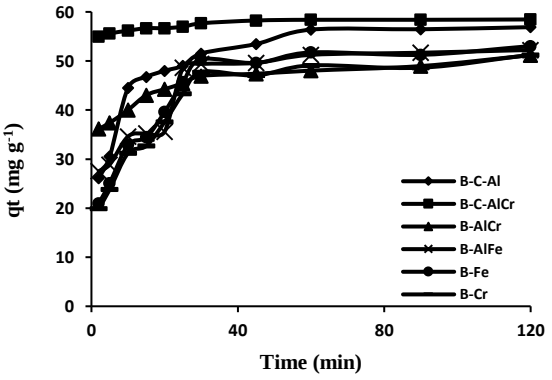

Fig.9: Effect of contact time on adsorption of E-4G onto modified bentonite samples.

The pseudo-first-order kinetic using the linear Lagergren equation is generally expressed as follows [46]:

$$\ln\left(q_e - q_t\right) = \ln q_e - k_1 t \qquad (11)$$

Where q_t is the amount adsorbed of dye at time t (mg/g) and k_1 is the rate constant of the pseudo-first-order model (min^{-1}). The k_1 and q_e calculated from the slope and intercept of plots ln (q_e-q_t) versus t, respectively are given in Table 3 and Fig. 10b. It was found that the correlation coefficients of the first-order model are lower than those of the pseudo-second-order model. This implies that the adsorption process does not follow the first-order kinetic model.

The pseudo-second order kinetic is expressed as follows [47]:

$$\frac{t}{q_t} = \frac{1}{k_2 q_e^2} + \frac{t}{q_e} \qquad (12)$$

Table 3: Kinetic parameters for the adsorption of E-4G onto modified bentonites.

Model	B-Fe	B-Cr	B-AlFe	B-AlCr	B-C-Al	B-C-AlCr
Pseudo-first order						
q_e (mg g^{-1})	34.64	03.46	34.64	12.00	32.52	03.33
k_1(min^{-1})	0.053	0.039	0.053	0.021	0.060	0.044
R^2	0.873	0.914	0.873	0.875	0.951	0.942
Pseudo-second order						
q_e (mg g^{-1})	55.55	55.60	55.56	50.00	58.82	58.83
k_2 (g(mg.min)$^{-1}$)	0.003	0.045	0.003	0.010	0.004	0.041
R^2	0.997	1.000	0.997	0.999	0.999	1.000
Intraparticle diffusion						
C(mg g^{-1})	47.09	51.54	45.88	42.54	55.14	58.02
k_p (mg(g.$min^{1/2}$)$^{-1}$)	0.506	0.116	0.604	0.738	0.152	0.047
R^2	0.699	0.972	0.927	0.924	0.816	0.844
qe_{exp} (mg g^{-1})	53.05	52.84	52.27	51.20	56.90	58.48

where k_2 is the rate constant of the pseudo-second-order model for the adsorption process (g/(mg.min)). Plots of t/q_t against t have been drawn in Fig. 10 a to obtain the rate parameters.

The kinetic data fit well the pseudo-second-order model with correlation coefficients higher than 0.999. The calculated q_e values of dye using the pseudo-second-order equation were found very close to the experimental q_e values, indicating that this kinetic model was very appropriate. The pseudo-second-order model is based on the assumption that the rate-limiting step may be chemisorption which involves valence forces through sharing or electron exchange between the adsorbent and the adsorbate [48]. As can be seen from Table 3, the values of k_2 for E-4G adsorption for all samples are similar, which means that the mobility rate of dye molecules has not changed from one adsorbent to the other.

The intraparticle diffusion equation can be written as follows [49]:

$$q_t = k_p t^{1/2} + C \quad (13)$$

where C is the intercept, and kp is the intraparticle diffusion rate constant (mg $g^{-1}min^{-1/2}$). The Plot q_t against the square root of time is shown in Fig. 10c.

According to this model, the plot of uptake, q_t, versus the square root of time ($t^{1/2}$) should be linear if the intraparticle diffusion is involved in the adsorption process; moreover, if this line passes through the origin, the intraparticle diffusion represents the rate-controlling step [50]. When the plots do not pass through the origin, this is indicative of some degree of boundary layer control, and this further shows that the intraparticle diffusion is not the only rate-limiting step, but there might be some other kinetic models that may control the adsorption rate, all these models may be operating simultaneously.

The results indicated in Table 3 suggest that the correlation coefficients (R^2) for the intraparticle diffusion model are 0.924, 0.927, and 0.972 for B-AlCr, B-AlFe, and B-Cr, respectively and the values of q_e calculated by this model was close to that of experimentally acquired q_e only in the case of B-Cr. This indicates that the adsorption of E-4G onto inorgano-bentonite samples may be followed by an intraparticle diffusion model for up to 25 minutes. However, the R^2 values for the other samples are very low, implying that some other mechanism along with intraparticle diffusion did play an important role in E-4G adsorption.

This suggests that the adsorption system studied belongs to the second-order kinetic model, based on the assumption that the rate-limiting step may be chemical sorption or chemisorption involving valence forces through sharing or exchange of electrons between adsorbent and adsorbate.

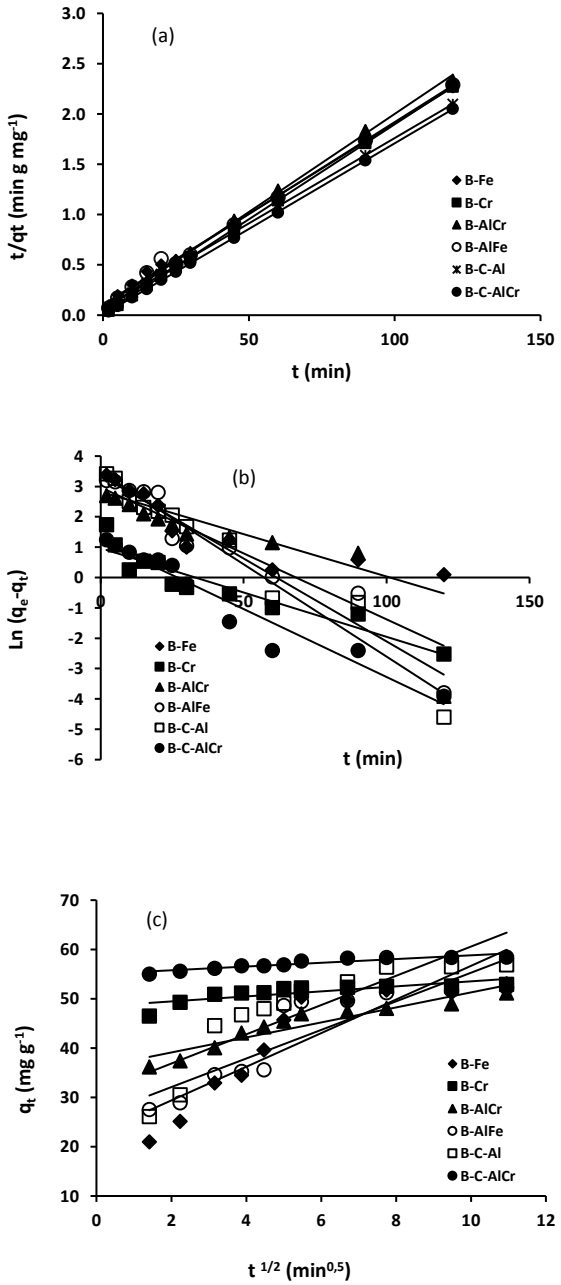

Fig.10: Plots of adsorption kinetic equations for adsorption of E-4G onto modified bentonites,(a) the pseudo-second-order,(b) the pseudo-first-order, and (c) the intraparticle diffusion equation.

Thermodynamic study

In order to calculate the heat or energy adsorption of E-4G dye onto modified bentonite, we carried out the adsorption reaction at 30, 40, and 50 °C for B-C-Al, B-C-AlCr, and B-AlFe samples, by using the following equations [51]:

$$\Delta G^\circ = \Delta H^\circ - T\Delta S^\circ \quad (14)$$

$$\ln K_d = \frac{-\Delta H^\circ}{R\,T} - \frac{\Delta S^\circ}{R} \quad (15)$$

$$K_d = \frac{q_e}{C_e} \quad (16)$$

Where $\Delta H°$, $\Delta S°$, $\Delta G°$ and T are the adsorption enthalpy, entropy, Gibbs free energy, and temperature in Kelvin, respectively. The slope and intercept of the curve of ln $K_d$versus $1/T$ correspond to $\Delta H/R$ and $\Delta S/R$, respectively.

The estimated thermodynamic parameters are depicted in Fig. 11 and the values of the heat adsorption are given in Table 4. The positive valueof $\Delta H°$ found in the case of B-AlFe suggests the endothermic nature of adsorption. Moreover, the positive value of $\Delta S°$implies increased randomness at the solid/solution interface during the removal of E-4G. Regarding the B-C-Al and B-C-AlCr samples, the negative values of $\Delta H°$ suggest the exothermic nature of adsorption. In addition, the negative value of $\Delta S°$entails that the dye molecules' disorder increases not at the interface but within the solution;it starts decreasing while approaching the solid surface. Similar results were observed for malachite green adsorption on the clayey soil of India [52].

The negative values of $\Delta G°$ for all samples studied are certainly due to the fact that the adsorption process is spontaneous; however, the adsorption spontaneity increases with the rising temperature only for inorgano-bentonite solid. Generally, the adsorption of acid dye E-4G onto pillared bentonite is favorable at room temperature and the reaction of adsorption is physic in nature.

CONCLUSIONS

The adsorbents employed in the present research were prepared by insertion of polycations solution of aluminum, iron, and chromium as well as cethytrimethyl cations into the purified bentonite. The pillared bentammoniumonites proved to be remarkable adsorbents that have a high capacity to remove E-4G dye from an aqueous solution.

Upon intercalation, the basal spacing of montmorillonite Mt in bentonite increased to 1.85 nm, in the case of cetyltrimethylammonium and aluminum intercalated bentonite (B-C-Al). The specific surface areas of the samples are also increased from 45 m^2/g of the natural bentonite to 122.2 and 141.4 m^2/g for B-C-Al and B-AlCr,

Table 4: Thermodynamic parameters for the adsorption of E-4G onto modified bentonites.

Sample	ΔH° (kJmol^{-1})	ΔS° (Jmol^{-1}K^{-1})	ΔG° (kJmol^{-1})			R^2
			30 °C	40 °C	50 °C	
B-C-Al	-7.943	-3.324	-6.935	-6.903	-6.869	0.973
B-C-AlCr	-12.573	-12.644	-8.735	-8.615	-8.489	0.986
B-AlFe	9.598	43.561	-3.601	-4.036	-4.471	0.931

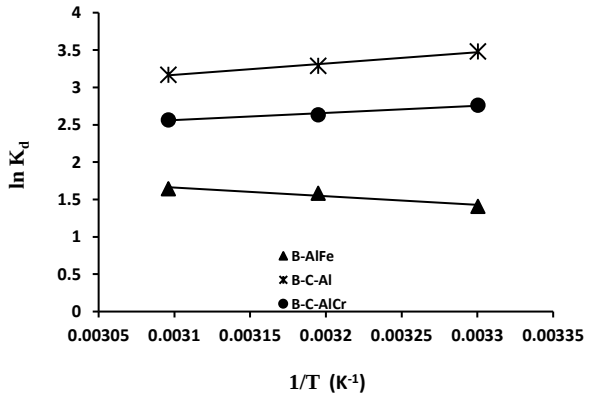

Fig.11: Plot K_d vs. 1/T for estimation of thermodynamic parameters for the adsorption of E-4G onto modified bentonites.

respectively. All these characterization parameters indicated the successful preparation of inorgano-bent and inorgano-organo-bent materials.

The adsorption behavior of acid dye onto pillared bentonites has been investigated while varying parameters such as pH, contact time, and temperature. The adsorption rates were rapid at the beginning of the process and then reached equilibrium after 60 minutes. The maximum dye removal is obtained for B-C-Al (385.25 mg/g) at the pH of the solution = 2 and at ambient temperature (25 °C). The adsorption of E-4G on pillared bentonite can be well described by pseudo-second-order. High correlation coefficient values (R^2 between 0.926 and 0.978) were found for the Freundlich isotherm, indicating that the adsorptions took place on a heterogeneous surface.

The negative values of $\Delta G°$ confirm a favorable adsorption process at all considered temperatures. The values of mean free energy obtained from Dubinin–Radushkevich (D–R) isotherm equation were below unit (E = 0.025-0.198), indicating that the adsorption process is physical in nature. In the end, it is worth noting that inorgano-organo-bent materials are potential low-cost *adsorbents*for the removal of E-4G dye from aqueous solutions, because they are easy to implement, and they can be applied within a wide rangeofpH values, and they have a high adsorption capacity.

Acknowledgments

The authors would like to warmly thank the Directorate General for Scientific Research and Technological Development (Algeria), the Ministry of Higher Education and Scientific Research (Algeria) for their financial assistance, as well as Pr. Jacques Schott GET laboratory (French), for his assistance with the analyses and characterization techniques.

Received : Jul.27, 2020 ; Accepted : Oct. 19, 2020

REFERENCES

[1] Mukhopadhyay R., Adhikari T., Sarkar B., Ranjan Paul A.B., Patra A.K., Sharma P.C., Kumar P., Fe-Exchanged Nano-Bentonite Out performs Fe_3O_4 Nanoparticles in Removing Nitrate and Bicarbonate from Wastewater, *J. Hazard. Mater.*, **376**:141-152 (2019).

[2] Chuekuna N., Wongchaisuwat A., Meesuk L., Zinc-8-hydroxyquinoline Intercalated in Calcium Bentonite: A Promising DO Sensor, *J. Phys. Chem. Solids*, **71**:423–426 (2010).

[3] Cheng H., Zhu Q., Xing Z., Adsorption of Ammonia Nitrogen in Low-Temperature Domestic Wastewater by Modification Bentonite, *J. Clean. Prod.*,**233**:720-730 (2019).

[4] Ahmad T., Guria C., Mandal A., Synthesis, Characterization and Performance Studies of Mixed-Matrix Poly(Vinyl Chloride)-Bentonite Ultrafiltration Membrane for the Treatment of Saline Oily Wastewater, *Process Saf. Environ.*, **116**: 703-717 (2018).

[5] Huang Z., Li Y., Chen W., Shi J., Zhang N., Xiaojin Wang, LiZ., GaoL., ZhangY., Modified Bentonite Adsorption of Organic Pollutants of Dye Wastewater, *Mater. Chem. Phy.*, **202**: 266-276 (2017).

[6] Ravaria M.H., Sarrafia A., Tahmooresi M., Synthesizing and Characterizing the Mixed Al, Cu-Pillared and Copper Doped Al-Pillared Bentonite for Electrocatalytic Reduction of CO_2, *S. Afr. J. Chem. Eng.*, **31**:1-6 (2020).

[7] Ayari F., Manai G., Khelifi S., Trabelsi-Ayad M., Treatment of Anionic Dye Aqueous Solution Using Ti, HDTMA and Al/Fe Pillared Bentonite. Essay to Regenerate the Adsorbent, *J. Saudi Chem. Soc.*, **23**:294-306 (2019).

[8] Laysandraa L., Kartika Saria M.W.M., Edi Soetaredjoa F., Foeb K., Putroc J.N., Kurniawanc A., Juc Y-H., Ismadj S., Adsorption and Photocatalytic Performance of Bentonite-Titanium Dioxide Composites for Methylene Blue and Rhodamine B Decoloration, *Heliyon*,**3**: e00488 (2017).

[9] Zahaf F., Dali N., Marouf R., Ouadjenia F., Schott J., Application of Hydroxy-Aluminum and Cetyltrimethylammonium Bromide-Intercalated Bentonite for Removing Acid and Reactive Dyes, *Desalination Water Treat.***57(44)**: 21045-21053 (2016).

[10] Tomul F., Adsorption and Catalytic Properties Fe/Cr-Pillared Bentonites, *Chem. Eng. J.*, **185-186**: 380-390 (2012).

[11] Belaroussi A., Labed F., Khenifi A., Ait Akbour R., Bouberka Z., Kameche M., Derriche Z., A Novel Approach for Removing an Industrial Dye 4GL by an Algerian Bentonite, *Acta Ecol. Sin.*, **38(2)**: 148-156 (2018).

[12] Chen Q., Wu P., Dang Z., Zhu N., Li P., Wu J., Wang X., Iron Pillared Vermiculite as a Heterogeneous Photo-Fenton Catalyst for Photocatalytic Degradation of Azo Dye Reactive Brilliant Orange X-GN, *Sep. Purif. Technol.*, **71**:315–323 (2010).

[13] Oyewo O.A., Elemike E.E., Onwudiwe D.C., Onyango M.S., Metal Oxide-Cellulose Nanocompositesfor the Removal of Toxic Metals and Dyes from Wastewater, *Int. J. Biol. Macromol.*, **164**:2477-2496 (2020).

[14] Zhou R., Zhou R., Zhang X., Bazaka K., Ostrikov K. K., Continuous Flow Removal of Acid Fuchsine by Dielectric Barrier Discharge Plasma Water Bed Enhanced by Activated Carbon Adsorption, *Front. Chem. Sci. Eng.*, **13(2)**: 340-349 (2019).

[15] Far H.S., Hasanzadeh M., Nashtaei M.S., Rabbani M., Haji A., Hadavi Moghadam B., PPI-Dendrimer-Functionalized Magnetic Metal-Organic Framework (Fe3O4@MOF@ PPI) with High Adsorption Capacity for Sustainable Wastewater Treatment, *ACS Appl. Mater. Interfaces*, **12(22)**: 25294-25303 (2020).

[16] Khosravi Mohammad Soltan F., Hajiani M., Haji, A., Nylon-6/poly (propylene imine) Dendrimer Hybrid Nanofibers: an Effective Adsorbent for the Removal of Anionic Dyes, *J. Text. Inst.*, 1-11 (2020).

[17] Qureshi R. F., Malik S.A., Qureshi K., Rajput A.W., Khatri Z., Bhatti I., Efficient Removal of Indigo Dye from Aqueous Solution by an Innovative Method of Emulsion Liquid Membrane, *Ind. Textile*, **69(6)**:472 (2018).

[18] Lima Beluci N.C., Affonso Pisano G.M., Sayury Miyashiro C., Cândido Homem N., Guttierres Gomesd R., Fagundes-Klenc M.R., Bergamasco R., Marquetotti Salcedo V.A., Hybrid Treatment of Coagulation/ Flocculation Process Followed by Ultrafiltration in TiO_2-Modified Membranes to Improve the Removal of Reactive Black 5 Dye, *Sci. Total Envir.*, **664**:222-229 (2019).

[19] Pradhan S.S., Konwar K., Ghosh T.N., Mondal B., Sarkar S.K., Deb P., Multifunctional Iron Oxide Embedded Reduced Graphene Oxide as a Versatile Adsorbent Candidate for Effectual Arsenic and Dye Removal, *Colloid Interface Commun.*, **39**: 100319 (2020).

[20] Alvi M.A., Shaheer Akhtar M., Effective Photocatalytic Dye Degradation Using Low Temperature Grown Zinc Oxide Nanostructures, *Mater. Letters*, **281**: 128609 (2020).

[21] Pourabadeh A., Baharinikoo L., Nouri A., Mehdizadeh B., Shojaei S., The Optimisation of Operating Parameters of Dye Removal: Application of Designs of Experiments, *Int. J. Environ. Anal. Chem.*, 1-10 (2019).

[22] Shojaei S., Shojaei S., Experimental Design and Modeling of Removal of Acid Green 25 Dye by Nanoscale Zero-Valent Iron, *Eur. Mediterr. J. Environ. Integ.*, **2(1)**: 15 (2017).

[23] Shojaei S., Ahmadi J., Davoodabadi Farahani M., Mehdizadehd B., Pirkamali M., Removal of Crystal Violet Using Nanozeolite-X from Aqueous Solution: Central Composite Design Optimization Study, *J. Water Environ. Nanotechnol*., **4(1)**: 40-47 (2019).

[24] Mehr H.V., Saffari J., Mohammadi S.Z., Shojaei S., The Removal of Methyl Violet 2B Dye Using Palm Kernel Activated Carbon: Thermodynamic and Kinetics Model, *Int. J. Environ. Sci. Technol*., **17**:1773-1782 (2020).

[25] Liang-Guo Y., Yuan-Yuan X., Hai-Qin Y., Xiao-Dong X., Qin W., Bin D., Adsorption of Phosphate From Aqueous Solution by Hydroxy-Aluminum, Hydroxy-Iron and Hydroxy-Iron–Aluminum Pillared Bentonites, *J. Hazard. Mater*., **179**: 244–250 (2010).

[26] Romero-Pérez A., Infantes-Molina A., Jiménez-López A., Jalil E. R., Sapag K., Rodriguez-Castellón E., Al-Pillared Montmorillonite as a Support for Catalysts Based on Ruthenium Sulfide in HDS Reactions, *Catal. Today*, **187**: 88–96 (2012).

[27] Zhu R., Wang T., Ge F., Chen W., You Z., Intercalation of Both CTMAB and Al13 into Montmorillonite, *J. Colloid Inter. Sci.*, **335**: 77–83 (2009).

[28] Khenifi A., Bouberka Z., Bentaleb K., Hamani H., Derriche Z., Removal of 2,4-DCP from Wastewater by CTAB/Bentonite Using One-Step and Two-Step Methods: A Comparative Study, *Chem. Eng. J.*, **146**: 345–354 (2009).

[29] Srivastava V.C., Mall I.D., Mishra I.M., Characterization of Mesoporous Rice Husk Ash (RHA) and Adsorption Kinetics of Metal Ions From Aqueous Solution onto RHA, *J. Hazard. Mater.*, **134**: 257–267 (2006).

[30] Navia R., "Environmental Use of Volcanic Soil as Natural Adsorption Materia"l, Ph.D. Thesis, University of Leoben, Austria (2004).

[31] Sears G., Determination of Specific Surface Area of Colloidal Silica by Titration with Sodium Hydroxide, *Anal. Chem*., **28**:1981–1983 (1956).

[32] Thomas S.M., Bertrand J.A., Occelli M.L., Huggins F., Gould S.A., Microporous Montmorillonites Expanded with Alumina Clusters and M[(μ-OH) Cu (μ-$OCH_2CH_2NEt_2$)]$_6$ (ClO_4)$_3$, (M = Al, Ga, and Fe), or Cr[(μ-OCH_3)(μ-$OCH_2CH_2NEt_2$) CuCl]$_3$ Complexes, *Inorg. Chem*., **38**: 2098–2105 (1999).

[33] Guo J., Chen S., Liu L., Li B., Yang P., Zhang L., Feng Y., Adsorption of Dye from Wastewater Using Chitosan–CTAB Modified Bentonites, *J. Colloid Interface Sci.*, **382**:61–66 (2012).

[34] Bulut E., Özacar M., Şengil I.A., Adsorption of Malachite Green onto Bentonite: Equilibrium and Kinetic Studies and Process Design, *Micropor. Mesopor. Mater.*,**115**: 234–246 (2008).

[35] Bouberka Z., Khenifi A., Ait Mahamed H., Haddou B., Belkaid N., Bettahar N., Derriche Z., Adsorption of Supranol Yellow 4 GL from Aqueous Solution by Surfactant- Treatedaluminum/Chromium-Intercalated Bentonite, *J. Hazard.Mater*., **162**:378–385 (2009).

[36] Gamoudi S., Srasra E., Adsorption of organic dyes by $HDPy^+$- Modified Clay: Effect of Molecular Structure on the Adsorption, *J. Mol. Struc.*, **1193**:522-531 (2019).

[37] Saloana Santos S.G., FrançaD. B., CastellanoL.R.C., Trigueiro P., Silva Filho E.C., SantosI. M.G., Fonseca M.G., Novel Modified Bentonites Applied to the Removal of an Anionic Azo-Dye from Aqueous Solution, *Colloid Surf. A Physicochem. Ang. Asp.*, **585**:124152 (2020).

[38] Giles C.H., MacEwan T.H., Nakhwa S.N., Smith D., Studies in Adsorption. Part XI: A System of Classification of Solution Adsorption Isotherms, and its Use in Diagnosis of Adsorption Mechanisms and in Measurements of Specific Surface Areas of Solids, *J. Chem. Soc*. **10**:3963–3973 (1960).

[39] Öncü-Kaya E.M., Şide N., Gök Ö., Özcan A.S., Özcan A., Evaluation on Dye Removal Capability of Didodecyldimethylammonium-Bentonite from Aqueous Solutions, *J. Disper. Sci. Technol*., **38(8)**: 1211-1220 (2016).

[40] Huang Z., Li Y., Chen W., Shi J., Zhang N., Wang X., Li Z., Gao L., Zhang Y., Modified Bentonite Adsorption of Organic Pollutants of Dye Wastewater, *Mater. Chem. Phy*., **202**: 266-276 (2017).

[41] Langmuir I., The Adsorption of Gases on Plane Surfaces of Glass, Mica and Platinum, *J. Am. Chem. Soc*., **40**: 1361–1403 (1918).

[42] Freundlich H.M.F., Über Die Adsorption in Lösungen, *Z. Phys. Chem*., **57**:385–470 (1906).

[43] Özcan A.S., Gök Ö., Structural Characterization of Dodecyltrimethylammonium (DTMA) Bromide Modified Sepiolite and its Adsorption Isotherm Studies, *J. Mol. Struct*., **1007**: 36–44 (2012).

[44] Dubinin M.M., Zaverina E.D., Radushkevich L.V., Sorption and Structure of Active Carbons. I. Adsorption of Organic Vapors, *Zh. Fiz. Khim*., **21**:1351–1362 (1947).

[45] Erdem B., Özcan A., Gok O., Özcan A.S., Immobilization of 2, 2-dipyridyl onto Bentonite and Its Adsorption Behaviour of Copper(II) Ions, *J. Hazard. Mater*., **163**:418–426 (2009).

[46] Ho Y.S., Citation Review of Langergren Kinetic Rate Equation on Adsorption Reactions, *Scientometrics*, **59**: 171–177 (2004).

[47] Ho Y.S., McKay G., The Kinetics of Sorption of Divalent Metal Ions onto Sphagnum Moss Peat, *Water Res*., **34**: 735–742 (2000).

[48] Wang L., Wang A., Adsorption Properties of Congo Red from Aqueous Solution onto Surfactant-Modified Montmorillonite, *J. Hazard. Mater*., **160**:173–180 (2008).

[49] Weber Jr W.J.., Morriss J.C., Kinetics of Adsorption on Carbon from Solution, *J. Sanitary Eng. Div. Am. Soc. Civ. Eng*, **89**:31–60 (1963).

[50] Bhattacharyya K.G., Sharma A., *Azadirachta indica* Leaf Powder as an Effective Biosorbent for Dyes a Case Study with Aqueous Congo Red Solutions, *J. Environ. Manage*., **71**:217–229 (2004).

[51] Chiou M.S., Li H.Y., Adsorption Behavior of Reactive Dye in Aqueous Solution on Chemical Cross-Linked Chitosan Beads, *Chemosphere*, **50**:1095–1105 (2003).

[52] Saha P., Chowdhury S., Gupta S., Kumar I., Insight into Adsorption Equilibrium, Kinetics and Thermodynamics of Malachite Green onto Clayey Soil of Indian Origin, *Chem. Eng. J.*, **165**: 874–882 (2010).